

# TEXTURE IN COLD ROLLED AND MAGNETICALLY AGED Fe–Mo–Ni–C ALLOYS

H.F.G. ABREU<sup>a</sup>, J.R. TEODÓSIO<sup>a</sup>  
and C.S. DA COSTA VIANA<sup>b,\*</sup>

<sup>a</sup>*Department of Metallurgical and Materials Engineering, Universidade Federal do Rio de Janeiro (UFRJ), C.P. 68505-Rio de Janeiro 21945-970, Brazil;* <sup>b</sup>*Department of Mechanical and Materials Engineering, Instituto Militar de Engenharia (IME), Rio de Janeiro 22290-270, Brazil*

(Received 10 July 1998)

The texture change due to the increase of cold rolling reduction in Fe–Mo–Ni–C alloys is described. Orientation Distribution Functions (ODF) for samples cold rolled 80%, 90%, 97% and 99% are shown and discussed. Below 90% cold rolling reduction, the texture in these alloys is similar to that of cold rolled low carbon steels. Above 90% cold rolling reduction, a decrease in the component {001}<110> is observed and the texture becomes weaker probably due to the development of shear bands. Magnetic age-annealing at 610°C for 1 h does not recrystallize completely these alloys. Samples cold rolled above 90% (97% and 99%) present an increase in the {001}<110> component, this being responsible for a corresponding increase in the magnetic anisotropy of these alloys.

**Keywords:** Cold rolling; Magnetic aging; Texture

## INTRODUCTION

Fe–Mo–Ni alloys are known for their high ductility and magnetic properties comparable to Vicalloy II (50% Co, 10–14% V and Fe). They have a BCC crystalline structure between room temperature and 1200°C (Jim and Tiefel, 1981) and their main advantage over Vicalloy II is the absence of the expensive element cobalt. The addition of carbon

---

\* Corresponding author. E-mail: d4viana@epq.ime.br.

improves their magnetic properties  $H_c$  (coercive force) and  $B_r$  (remanence) (Tavares *et al.*, 1994) through the formation of the carbides  $M_6C$ , where M is either Fe or Mo (Tavares *et al.*, 1995).

Magat *et al.* (1988) and Lujinskaia *et al.* (1984) showed that severe cold deformation of Fe–20Mo–5Ni alloys prior to magnetic aging improves  $B_r$  and  $H_c$ . They suggested that the magnetic anisotropy introduced by cold deformation is a result of crystallographic texture development in the material. Later, Abreu *et al.* (submitted) confirmed that cold rolling in excess of 80% does introduce magnetic anisotropy in these alloys. Their work also showed that a sharp  $\{001\}\langle 110 \rangle$  texture component appears after magnetic aging and increases with the amount of previous cold rolling reduction. It was concluded that the magnetic anisotropy was linked to the increase in the volume fraction of that component.

In this work, the texture introduced in an Fe–20Mo–5Ni alloy with different carbon contents by cold rolling and, cold rolling and age-annealing is analyzed. The magnetic anisotropy is measured and related to the texture components identified. The textures developed in low carbon steels by cold rolling and annealing are used for comparison.

## EXPERIMENTAL

Fe–Mo–Ni–C ingots were prepared by induction melting under vacuum. The compositions of the ingots are shown in Table I. The ingots were soaked at 1250°C for 30 min and then 60% hot rolled in one pass. The strips were reheated to 1250°C and quenched in water. The hot-rolled-and-quenched strips were cold reduced by 80%, 90% and 97%. An extra specimen reduced by 99% was prepared for the material with 0.020% C taking advantage of the high ductility displayed by this alloy. The magnetic age-annealing treatment was carried out at 610°C for 1 h.

Incomplete pole figures were measured on ground and chemically polished 20 mm × 14 mm rectangles cut from the rolled and treated

TABLE I Chemical composition of the alloys in weight percent

<i>Alloy</i>	<i>C</i>	<i>Ni</i>	<i>Mo</i>	<i>Mn</i>	<i>Co</i>	<i>Fe</i>
A	0.020	5.00	20.3	0.16	< 0.01	bal.
B	0.057	5.00	19.3	0.12	< 0.01	bal.
C	0.092	5.07	19.0	—	< 0.01	bal.

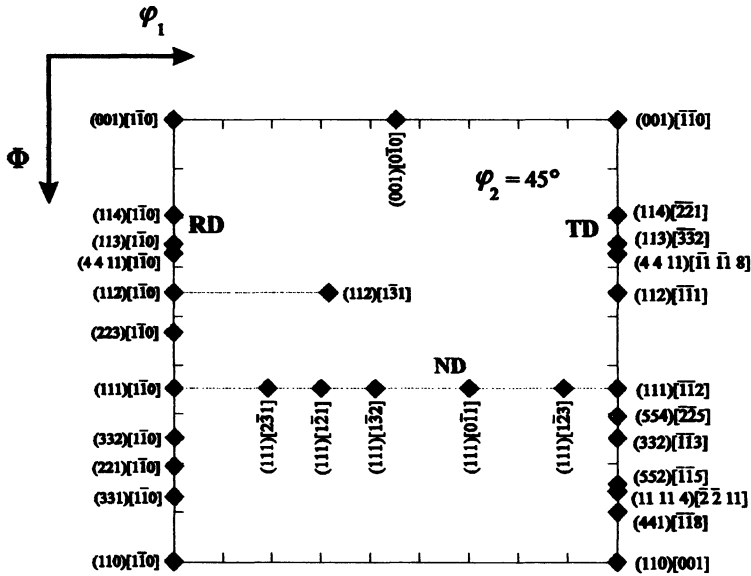


FIGURE 1  $\varphi_2 = 45^\circ$  orientation chart showing the position of the main orientations along with the RD-, TD- and ND-fibers.

materials. The method of Schultz was used with  $\text{CoK}_\alpha$  radiation and the intensities were corrected for background and defocalization.

The crystallographic texture was determined by calculating the orientation distribution function (ODF) using Roe's method (Roe, 1965). The ODFs were computed from measured  $\{110\}$ ,  $\{200\}$  and  $\{211\}$  incomplete pole figures by fitting a harmonic series expanded to  $l = 22$ . The orientation densities were represented by  $\varphi_2 = 45^\circ$  Bunge (Bunge, 1993) sections and along special fibers in the Euler space. Figure 1 shows the  $\varphi_2 = 45^\circ$  orientation chart in Bunge's coordinates containing the relevant texture components. The lines marked with RD, TD and ND represent fibers with  $\langle 110 \rangle$  parallel to the rolling direction,  $\langle 110 \rangle$  parallel to the transverse direction and  $\langle 111 \rangle$  parallel to the normal direction, respectively.

## RESULTS

Figure 2 shows the  $\varphi_2 = 45^\circ$  ODF sections for alloy B in the conditions: (a) 60% hot rolled and water quenched, and (b) 60% hot rolled, solution

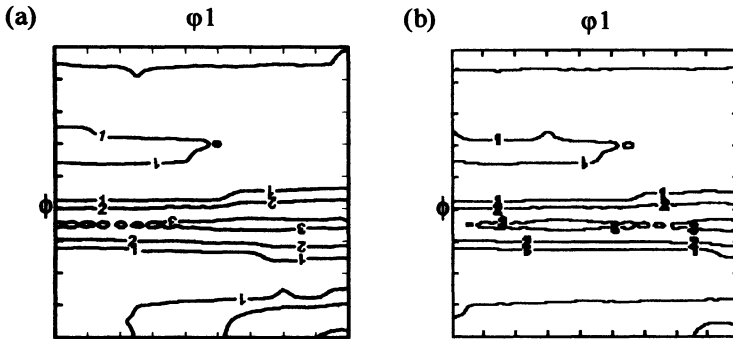


FIGURE 2  $\varphi_2 = 45^\circ$  ODF sections for alloy B (a) hot rolled 60% and (b) solution treated at 1220°C followed by water quenching.

treated at 1250°C and water quenched. It can be seen that the major difference introduced by the solution treatment lies in the slight decrease in the intensity of the (110)[001] component for the solution treated and quenched condition.

Figure 3 shows the  $\varphi_2 = 45^\circ$  ODF sections of alloys A, B and C cold rolled 80%, 90%, 97% and 99% (only for alloy A). For the three alloys the texture is sharpest at 90% reduction. The main texture components are the (001)[110], the (001)[1 $\bar{1}$ 0] and the (111)[0 $\bar{1}$ 1]. For the more severe reductions, 97% and 99% (for alloy A), the intensities of these components are observed to decrease and a better defined ND-fiber is developed.

Figures 4 and 5 show the behaviors of the components with  $\langle 110 \rangle$  directions parallel to RD and TD, i.e. the RD- and TD-fibers, respectively, for alloys A, B and C, for different rolling reductions. The  $\{111\}\langle 110 \rangle$  and  $\{111\}\langle 112 \rangle$  orientations, the main components of the ND-fiber, were also included in these graphs, accordingly. The components in the RD-fiber increase in intensity from 80% to 90% deformation and then decrease for higher reductions. The reason for this decrease is thought to be the appearance of shear bands in the samples deformed 97% and 99% (this possibility is currently being investigated.). Mathur and Backofen (1973) reported that shear bands are not observed in Al-killed steels below about 90% rolling reduction. Above 90%, however, these bands apparently introduce marked alterations in the deformation texture.

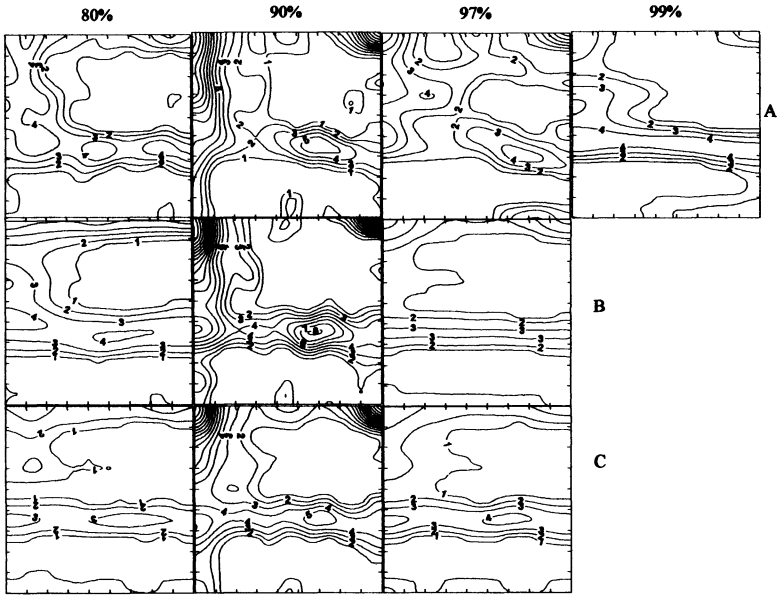


FIGURE 3  $\varphi_2 = 45^\circ$  ODF sections of alloys A, B and C for different cold rolling reductions steels.

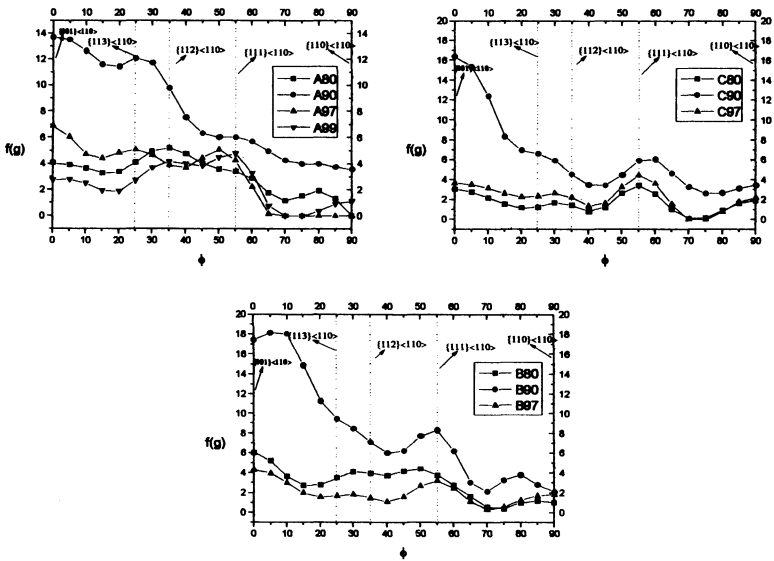


FIGURE 4 RD-fiber representation of the influence of cold rolling reduction on the deformation texture of Fe-20Mo-5Ni-C alloys.

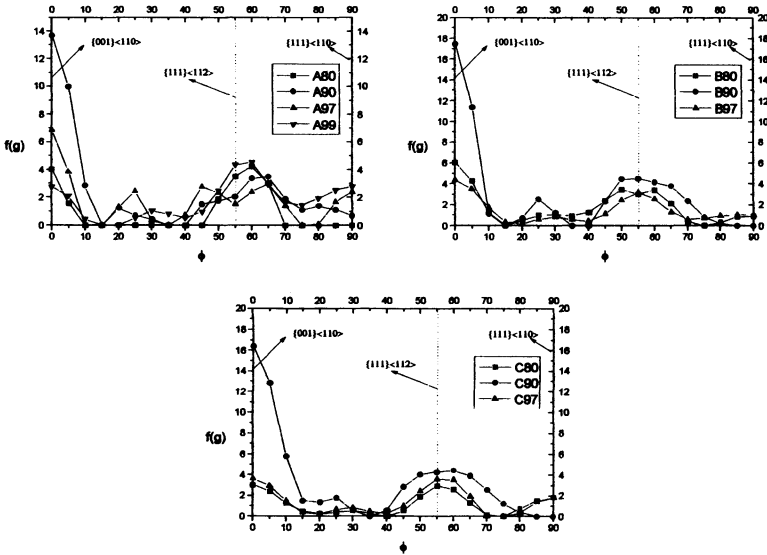


FIGURE 5 TD-fiber representation of the influence of cold rolling reduction on the deformation texture of Fe-20Mo-5Ni-C alloys.

Figure 6 shows the  $\varphi_2 = 45^\circ$  ODF sections of alloys A, B and C cold rolled and magnetically age-annealed for 1 h at  $610^\circ\text{C}$ . The main texture components are  $\{100\}\langle 110\rangle$  and  $\{111\}\langle 110\rangle$ . The  $\{001\}\langle 110\rangle$  components show an increasing value of intensity for rolling reductions in excess of 90%. This is an important trend since it also leads to an increase in the magnetic anisotropy of these alloys on account of the  $\langle 100\rangle$  directions – the direction of easiest magnetization – lying in the TD direction. This is especially useful in the case of thin gauge materials for magnetic core applications.

Figures 7 and 8 show respectively the behaviors of the components in the RD- and FD-fibers, taken from Fig. 6. In Fig. 7, the joint effect of carbon content and rolling reduction on the growth of the near- $\{111\}\langle 110\rangle$  orientations can be easily noted. This is clearer for alloys B and C, the latter having the highest carbon content. Optical metallography of these samples showed that, even after magnetic age-annealing, recrystallization was still incomplete.

Figure 9 shows the  $\varphi_2 = 45^\circ$  sections of alloy A in the conditions: (a) cold rolled 90%; (b) cold rolled 90%, heat treated at  $1200^\circ\text{C}$  for 3 mins

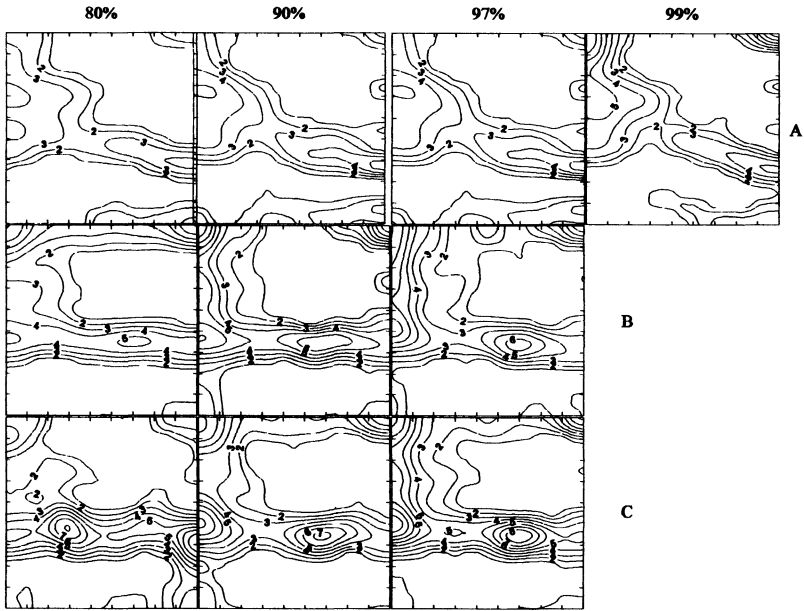


FIGURE 6  $\varphi_2=45^\circ$  ODF sections of the textures of alloys A, B and C after magnetic aging at  $610^\circ\text{C}$  for 1 h.

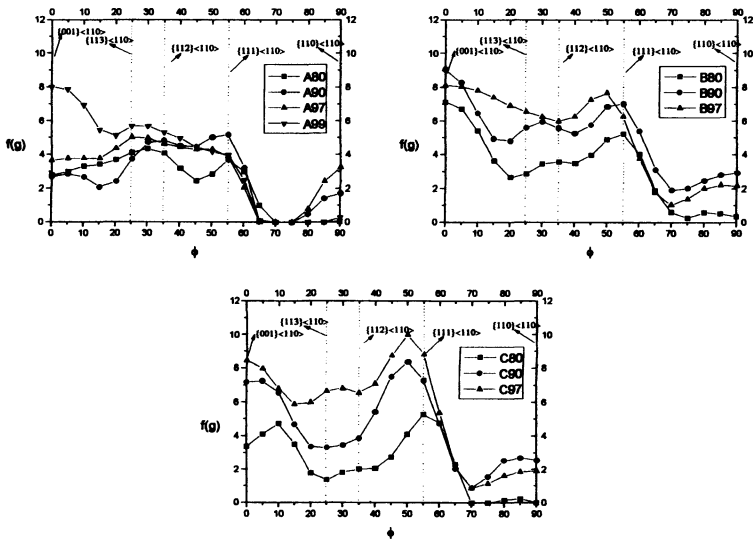


FIGURE 7 RD-fiber representation of the influence of cold rolling reduction on texture of the magnetically aged Fe-20Mo-5Ni-C alloys.

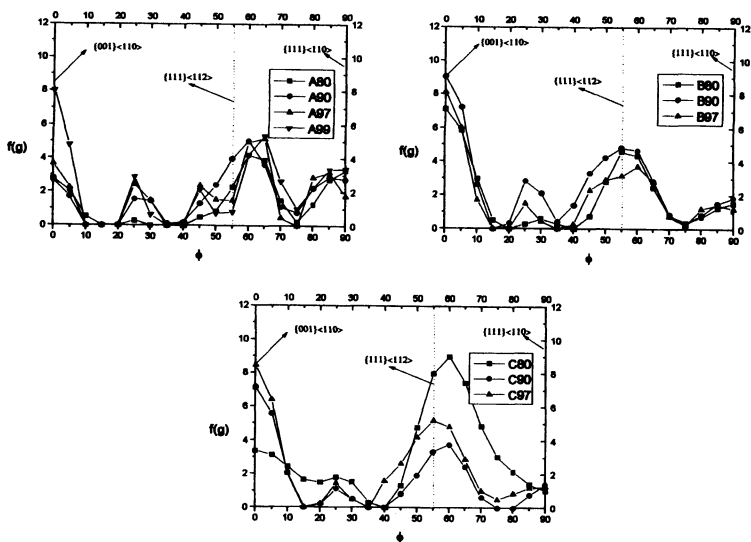


FIGURE 8 TD-fiber representation of the influence of cold rolling reduction on texture of the magnetically aged Fe-20Mo-5Ni-C alloys.

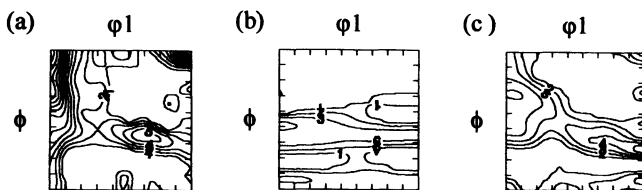


FIGURE 9  $\varphi_2 = 45^\circ$  ODF sections of the alloy Fe-20Mo-5Ni-0.02C cold rolled 90%, solution treated at 1200°C and quenched in water.

and quenched in water; and (c) cold rolled 90% and magnetically aged at 610°C for 1 h. It can be seen that the age-annealing texture of Fe-Mo-Ni-C alloys is characterized by the presence of an ND-fiber in the same fashion as that observed in low carbon steels.

Figure 10 (Heckler and Granzow, 1970) shows the  $\varphi = 45^\circ$  sections of a low carbon steel cold rolled 60% and annealed at different temperatures. Recrystallization starts near 566°C and by 738°C it is already complete. The similarity between these textures – both in the cold rolling and the recrystallized conditions – and those in the corresponding conditions for the Fe-20Mo-5Ni-C alloys, shown above, is readily noticed. This



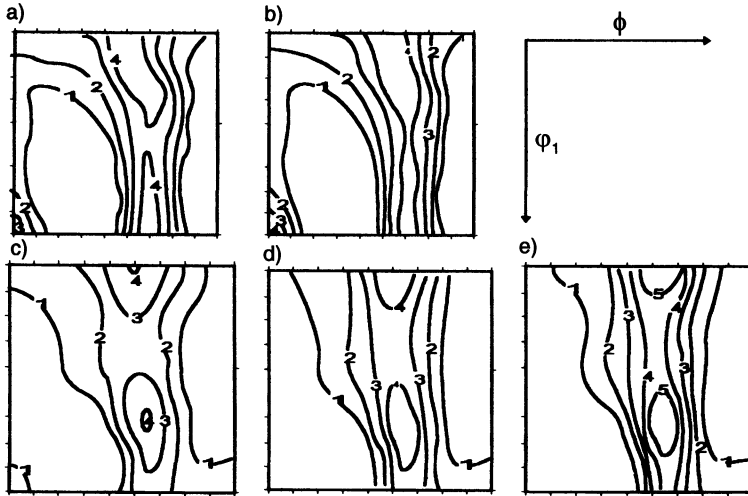


FIGURE 10  $\phi = 45^\circ$  Roe sections for a low-carbon steel (a) cold rolled 60%; cold rolled 60% and annealed at: (b) 468°C, (c) 538°C, (d) 566°C and (e) 738°C, respectively (Heckler and Granzow, 1970).

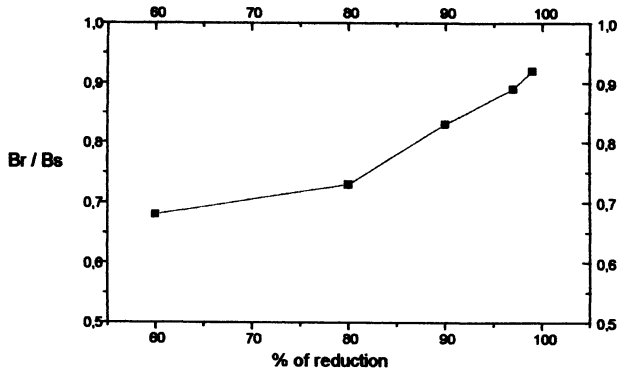


FIGURE 11 Magnetic anisotropy ratio  $B_r/B_s$  for alloy N as a function of cold rolling reduction.

suggests that both the deformation and the annealing mechanisms that take place in the present alloy are similar to those in carbon steels.

The ratio between magnetic remanence ( $B_r$ ) and magnetic saturation induction ( $B_s$ ) is used to quantify the magnetic anisotropy of a material. When this ratio is higher than 0.8 the material is said to be magnetically anisotropic. Figure 11 shows the variation of the ratio  $B_r/B_s$ , with rolling

reduction for alloy A. It can be seen that this alloy becomes magnetically anisotropic for rolling reductions in excess of about 87%, which virtually coincides with the reduction at which the texture alterations were noticed, as pointed out above.

## CONCLUSIONS

The crystallite orientation distribution function analysis was used to study the development of cold rolled, and cold rolled and magnetically age-annealed Fe–20Mo–5Ni–C semi-hard magnetic alloys. With increasing cold rolling reduction, Fe–20Mo–5Ni–C alloys exhibit the simultaneous development of a partial  $\langle 110 \rangle$  fiber axis parallel to rolling direction, with main components  $\{100\}\langle 110 \rangle$ ,  $\{111\}\langle 110 \rangle$  and a  $\langle 111 \rangle$  fiber parallel to the normal direction. Below 90% cold rolling reduction, this texture development is similar to that of cold rolled low carbon steels. Above 90% cold rolling reduction, a decrease in the component  $\{001\}\langle 110 \rangle$  takes place and the texture becomes weaker probably due to the development of shear bands. Magnetic age-annealing at 610°C for 1 h does not recrystallize completely these alloys. Samples cold rolled 80% and 90% show a reduction in the  $\{001\}\langle 110 \rangle$  component. Samples cold rolled 97% and 99% present an increase in the  $\{001\}\langle 110 \rangle$  component and this is responsible for the magnetic anisotropy of these alloys. The recrystallization textures of these alloys are similar to those found in low carbon steels.

## References

- Abreu, H.F.G., Teodosio, J.R., Neto, J.M. and Silva, M.R. Texture development and magnetic anisotropy in semi-hard magnetic Fe–20Mo%Ni–C magnetic alloys: submitted to *Scripta Metall.*
- Bunge, H.J. (1982) *Texture Analysis in Material Science, Mathematical Methods* Butterworths publ. London. 2nd Edition, Cuvillier Verlag, Göttingen, 1993.
- Heckler, A.J. and Granzow, W.G. (1970) Crystallite orientation distribution analysis of the cold rolled and recrystallization textures in low-carbon steels. *Metallurgical Transaction*, **1**, 2089–2094.
- Jim, S. and Tiefel, T.H. (1981) New ductile Fe–Mo–Ni magnet alloys. *Journal of Applied Physics*, **52**(3).
- Lujinskaia, M.G., Chilova, N.F. and Chur, I.S. (1984) *Fis. Metal Metaloved*, **57**, 1075.
- Magat, E.M., Makarov, G.M., Lapina, L.P. and Beloterov, E. (1988). *Fis. Metal Metaloved*, **55**, 1075.

- Mathur, P.S. and Backofen, W.A. (1973) Mechanical contributions to plane-strain deformation and recrystallization textures of aluminum-killed steel. *Metallurgical Transaction*, **4**, 643–651.
- Roe, R.J. (1965) *J. Appl. Phys.*, **36**, 2024.
- Tavares, S.M., Moura, M.P. and Teodósio, J.R. (1994) Magnetic properties of an Fe-20Mo-5Ni-0.12C alloy. *Journal of Magnetism and Magnetic Materials*, **137**, 103–106.
- Tavares, S.M., Pires, M.M. and Teodósio, J.R. (1995) Microstructural features of a Fe-20Mo-5Ni-0.12C magnetic alloy. *Scripta Metallurgica e Materialia*, **33**, 251–257.